

# IMPROVING GROUND MOVING TARGET INDICATION PERFORMANCE

*Nicholas Pulsone, Charles Rader and Bipin Mathew*

Massachusetts Institute of Technology Lincoln Laboratory  
244 Wood Street, Lexington, MA 02420

pulsone@ll.mit.edu    rader@ll.mit.edu    mathewb@ll.mit.edu

## ABSTRACT

*Lincoln Laboratory is investigating several concepts to improve airborne Ground Moving Target Indication (GMTI) performance as part of the Knowledge Aided Sensor Signal Processing and Expert Reasoning (KASSPER) Program. Some of these concepts incorporate ideas currently used for synthetic aperture radar (SAR) imagery and these require longer coherent processing intervals (CPIs) than what is typical for GMTI processing. Other concepts are more general and are applicable to any processing interval (long or short). This paper examines these concepts in detail and demonstrates their utility with synthetic radar data and actual data collected with the Tuxedo sensor.*

## 1. INTRODUCTION

Intelligence, Surveillance and Reconnaissance (ISR) systems are faced with a formidable task of locating and tracking all ground-based vehicles within the coverage area of the radar. Typically stationary vehicles are located with synthetic aperture radar (SAR) imagery and moving targets are located and tracked with Ground Moving Target Indication (GMTI). Most GMTI architectures employ a technique to reduce clutter such as the displaced phase center array (DPCA) technique or space-time adaptive processing (STAP). In general STAP provides better clutter nulling capabilities than the DPCA technique [1]. However, simplifying assumptions are often made in the development of STAP algorithms, such as homogeneous clutter and target-free training data. Unfortunately, in modern military applications existing ISR systems are faced with complex heterogeneous clutter, clutter discretets and dense target environments, causing false alarms and missed detections. As a result, in some scenarios the performance of existing STAP and constant false alarm rate (CFAR) algorithms may fall short of what is predicted by theory. The most challenging problem for GMTI systems is the detection and tracking

of *slow movers* – targets with a small velocity component along the radar line of sight.

These GMTI shortcomings are currently under investigation by Lincoln Laboratory as part of the KASSPER Program. In this paper we explore several algorithm concepts to improve GMTI performance. Recently, there has been interest in concepts that involve synergies between GMTI and SAR processing modes. A typical GMTI radar mode is characterized with a relatively large aperture, narrow bandwidth and short CPI duration. As such, we can represent GMTI modes in the red shaded area in Figure 1. In contrast a typical SAR radar mode is characterized with a relatively small aperture, wide bandwidth and long CPI duration. Hence we can represent SAR modes in the blue shaded area in Figure 1. As previously mentioned ISR systems use GMTI radar modes to locate moving targets and use SAR imagery to locate stationary targets. An intuitive compromise for locating slow moving targets is highlighted in the green shaded area. In Section 4 we explore this space by considering a CPI duration much longer than what is typically used in GMTI. By adopting a longer GMTI CPI length we must consider range and Doppler walk. In fact the concept we explore in Section 4 will exploit the difference in Doppler walk between stationary clutter and ground moving targets to identify slow movers.

In Section 5 we introduce a variation on *power selective training* [2] which we call *power variable training*. Our approach addresses the overnulling nature of *power selective training*. Section 6 describes a multi-channel adaptive SAR technique developed for the Foliage Penetration (FOPEN) Program [3] to detect ground moving vehicles below tree canopies. The principles in this technique are general and can also be applied to other GMTI systems. In Section 7 we describe the *extended array receiver* concept that provides narrow two-way (transmit and receive) beampatterns over a wide coverage area. Finally in Section 8 we conclude with a summary.

---

This work is sponsored by the Defense Advanced Research Projects Agency, under Air Force Contract F19628-00-C-0002. Opinions, interpretations, conclusions, and recommendations are those of the authors and are not necessarily endorsed by the United States Government.

## 2. BASELINE STAP

In a previous paper [4] we introduced a baseline GMTI processing architecture for the KASSPER Program. The baseline GMTI processing stream consists of five operations:

1. adaptive beamform,
2. pulse compression,
3. Doppler filter,
4. STAP and
5. detection.

The adaptive beamform operation suppresses unwanted interference appearing in the radar system frequency band and reduces the number of spatial degrees-of-freedom (DOF). Pulse compression is performed in the usual manner by convolving the pulse compression filter weights with the incoming range samples. Doppler filtering is performed using two FFT operations, one for pulses  $1 \dots N - 1$ , (where  $N$  is the number of pulses in the CPI) and the other for pulses  $2 \dots N$ . This Doppler filtering process prepares the data for a post-Doppler PRI-staggered STAP operation [1]. The training strategy for this baseline STAP operation chooses equally-spaced range samples within each Doppler bin. From this training set, the sample estimate of the covariance matrix is computed with a diagonal loading term selected to satisfy a white noise gain constraint [5]. The final operation consists of a sliding split-window greatest-of excision CFAR algorithm followed by an adaptive sidelobe blanker operation [6].

## 3. TUXEDO DATA

Some of the KASSPER signal processing concepts proposed by Lincoln Laboratory are based on an extended GMTI CPI-length (greater than 250 msec). To evaluate GMTI processing concepts involving these longer CPIs we are using data collected with the Tuxedo sensor in May of 1999 at Camp Navajo, Arizona. The Tuxedo Sensor is an experimental airborne X-band radar system, operated by Lockheed Martin, that is capable of recording digitized data in a variety of SAR and GMTI modes. During the data collection events at Camp Navajo the Tuxedo Sensor recorded data from all three phase centers in the antenna array for approximately a minute. In these events five military vehicles equipped with GPS sensors drove on a network of roads while recording their position (see Figure 2). The long recording intervals, SAR imagery and vehicle ground truth make the Tuxedo data set suitable for evaluating several of our advanced GMTI concepts. In Table 3 we list the pertinent system parameters for the Tuxedo sensor in its low resolution GMTI mode of operation.

Figures 3, 4 and 5 depict outputs from the baseline processing stream using the Tuxedo data. The specific data set

Table 1: System Parameters for the Tuxedo Sensor

Parameter	Value
Center Frequency	9.6 GHz
Bandwidth	66 MHz
PRF	1,400 Hz
Number of Transmit Apertures	1
Number of Receive Apertures	3
Azimuth Beamwidth Aperture	$3.6^\circ$
Elevation Beamwidth Aperture	$9.1^\circ$
Polarization	HH
A/C Heading	$290^\circ$
Depression Angle	$15^\circ$
Recorded Time	$\approx 1$ minute

processed has been designated by Lockheed Martin as Pass Number 1960. In this data set five military vehicles traveled at low speeds, approximately 5 mph, in the grid of roads designated in Figure 2. Figure 3 depicts the power from one of the three sensor channels after Doppler processing using 512 consecutive pulses of data. As expected there are strong radar returns from building roof-tops and other clutter discretely at lower Doppler speeds. Figure 4 depicts the output power after the PRI-staggered STAP operation. The dark vertical stripes in this figure correspond to Doppler bins in which the training data contained significant contributions from clutter discretely. For these Doppler bins the resultant adaptive weight vector overnulls the clutter and produced the low power outputs. In many of the remaining lower speed Doppler bins the clutter discretely appearing in Figure 3 were not suppressed sufficiently by the STAP operation and are still visible in Figure 4. Finally in Figure 5 we illustrate the output data after the CFAR normalization process. The detections and false alarms are each marked with a large 'x' superimposed over the range-Doppler cells that remain after the adaptive sidelobe blanking operation. T, F, and H mark the range where there are actual targets (Two-ton truck, Fuel truck and HMMWV) to detect. Notice there are many false alarms due to the clutter discretely in the Camp Navajo area. The stream of detections at approximately 22.6 kilometers in range corresponds to reflections from a train that happened to pass through the targeted area at the same time radar data was recorded.

The results in this section are probably typical of GMTI systems that make no use of any prior knowledge of the sort that we wish to exploit in the KASSPER program.

## 4. MOVING TARGET FOCUSING

This section describes a concept for improving GMTI performance using an approach adopted from SAR imaging of moving targets [7]. Typical SAR image processing focuses energy using a stationary target model. Targets moving in

the cross-range direction will appear smeared and result in significant losses in target-to-clutter power, see Figure 6. The techniques proposed in [7] refocuses the SAR image based on the velocity of the moving target, see Figure 7. Obviously in a practical application we do not know the target velocity a priori, therefore, several refocused images may be required to detect the range of speeds typical for ground moving vehicles. A similar approach can be used in GMTI processing when the CPI is long. We call this approach *moving target focusing*.

A derivation for this approach proceeds as follows. Consider an airborne GMTI platform with a side-looking array moving with velocity  $v_{AX}$  in the cross-range direction. Also consider a ground moving vehicle moving at constant speed. Designate the ground target cross-range velocity component as  $v_{TX}$  and slant-range velocity component as  $v_{TS}$ . We use these velocity components to define a new quantity,

$$\gamma = \sqrt{(v_{AX} - v_{TX})^2 + v_{TS}^2}. \quad (1)$$

that represents the norm of the relative velocity vector between the airborne platform and the ground moving target. If we assume the ground target moves with constant velocity and is located at a range  $R$  at time  $t = 0$  then expressions for range and range rate (or Doppler velocity) are given as follows,

$$r(t) = \sqrt{R^2 + 2Rv_{TS}t + \gamma^2 t^2} \quad (2)$$

$$\dot{r}(t) = \frac{Rv_{TS} + \gamma^2 t}{r(t)}. \quad (3)$$

For shorter CPIs (on the order of tens of milliseconds) and narrow bandwidth waveforms (between 10-20 MHz) range walk and Doppler walk of the target is negligible. In fact, for GMTI waveforms with these characteristics it is convenient to approximate the range of the ground moving target as  $r(t) \approx R$  and the range rate as  $\dot{r}(t) \approx v_{TS}$ . However, by adopting a longer GMTI CPI we must consider the effects of range walk and Doppler walk.

Consider a longer GMTI CPI, on the order of one second (a ground moving target is typically considered coherent for up to a second). For a narrow bandwidth, say  $BW = 10$  MHz, and a hamming weighted pulse compression filter the range resolution is given by

$$\Delta r = \frac{1.81 c}{BW} \frac{c}{2} \approx 27m. \quad (4)$$

where  $c$  is the speed of light. Assuming a ground target has a maximum range rate of about 25 m/sec then over a processing interval of one second the ground target does not traverse more than two range resolution cells. Consequently, it is fair to assume the effects of range walk are minimal. In ongoing research we would like to consider wider bandwidths for which range walk is no longer negligible.

Assuming a hamming weighted Doppler filter operation, the Doppler resolution for a CPI of duration  $T$  is given by

$$\Delta \dot{r} = \frac{1.81 \lambda}{T} \frac{\lambda}{2}. \quad (5)$$

where  $\lambda$  is the wavelength. Doppler walk can be neglected if the range rate of the ground target does not change more than the Doppler resolution over the CPI duration  $T$ , alternatively for large  $R$ ,

$$T < \sqrt{\frac{1.81 R \lambda}{\gamma^2} \frac{\lambda}{2}}. \quad (6)$$

Figure 8 plots the limit on CPI time for Doppler walk given in equation (6). The three curves represent different ground target velocities. Notice, even at a slant range of 60 km the CPI time limit is less than a quarter of a second. Therefore for a one second CPI time there is considerable Doppler walk over the CPI.

Figure 9 plots the number of Doppler resolution cells that a broadside target traverses in a one second interval. Again, there are three curves representing different target velocities. The middle curve represent stationary targets and the other two curves represent moving targets. The differences in the number of Doppler resolution cells in the three curves represents the phenomenon we would like to exploit in *moving target focusing*.

A target's Doppler walk over several Doppler resolution cells can be corrected (or focused) such that the target appears in a single Doppler resolution cell. For a narrowband waveform we are able to correct for Doppler walk with the following complex multiplier on each pulse in the CPI

$$\exp \left[ \frac{j2\pi\gamma^2 t^2}{\lambda R} \right]. \quad (7)$$

From equation (7) we see that the correction term varies with the target velocity or  $\gamma$ . The moving target focusing concept involves refocusing the radar data for different target velocity hypotheses to determine if a target is stationary (i.e. clutter) or moving.

For maximum signal-to-noise ratio (S/N) we would like to correct for each possible  $\gamma$  but this is costly. Figure 10 illustrates the response for a bank of five focusing filters over a range of  $\gamma$  or target velocities. Note that the S/N for a target can vary more than 7 dB depending on the target velocity but this variation can be kept to only 1 dB by choosing the best among five different corrections. This property can be used to distinguish moving targets from stationary targets by examining the outputs of the filter bank. Alternatively, it has been noted in [10] that the focus of moving targets in SAR images may be obtained with higher order moments of the phase error. What is remarkable about this concept is that we are able to distinguish targets that move

in *cross-range* from stationary targets. Recall that traditionally GMTI processing enables us to detect targets that move in *slant-range*. Thus moving target focusing provides a new capability for detecting moving targets which are not otherwise detectable with traditional GMTI processing.

## 5. POWER VARIABLE TRAINING

Power selective training is an appealing STAP training method for airborne moving target indication (AMTI) [2]. But power selected training leads to *overnulling* which increases the minimum detectable velocity. This is acceptable in the AMTI problem since most airborne targets typically move at considerable speeds, but it is undesirable in the GMTI application. However, we can get the advantages of power selective training in a GMTI processor without overnulling by using a more intelligent and effective STAP training method. We call this new technique *power variable training without over-nulling*.

Consider the notional plot in Figure 11, which represents the received radar power as a function of range for a given Doppler bin. For a multi-channel radar receiver this plot represents the total received power across all channels. If we define  $x_i(r)$  to represent the complex voltage received on the  $i^{th}$  channel for the  $r^{th}$  range resolution bin then the plot in Figure 11 depicts  $e(r) = \sum_i x_i(r)x_i(r)^*$  where  $*$  denotes complex conjugate. In power variable training we initially choose candidate training data from the  $K$  range samples that correspond to the largest values of  $e(r)$ , highlighted in red on Figure 11.

Subsequently, we estimate the angle of arrival for each of the candidate training samples and determine which samples are close in angle to what is predicted for main beam clutter. Those training samples whose angle estimates are close to the predicted angle for clutter are retained while all others are rejected. A similar rejection procedure is described in [8]. The remaining  $K'$  training samples, where  $K' \leq K$ , are used to estimate the following clutter-only covariance,

$$\mathbf{R}_c = \frac{1}{K'} \sum_{i=1}^{K'} \mathbf{x}_i \mathbf{x}_i^H - \sigma^2 \mathbf{I} \quad (8)$$

where  $^H$  denotes complex conjugate transpose. The matrix  $\sigma^2 \mathbf{I}$  on the right-hand side of equation (8) represents an estimate of the covariance matrix of the system noise, in this manner  $\mathbf{R}_c$  represents an estimate of the clutter alone devoid of system noise.

In the conventional power selected training, we would have used  $\mathbf{R}_c$  as the estimated covariance matrix, with some diagonal loading. But in the power variable training approach we vary the scale of  $\mathbf{R}_c$  according to the energy in the sample we are going to try to null.

As indicated in Figure 11, for a given Doppler bin we “tile” the dynamic range of  $e(r)$  into different power levels. For each “tile” or range of energy levels we compute a different adaptive weight vector whose clutter null depth matches the clutter power in that tile. Specifically, for tile  $m$  we first compute the scalar

$$\beta_m = \frac{\bar{e}_m - \sigma^2 N}{\text{tr}[\mathbf{R}_c]} \quad (9)$$

where  $\bar{e}_m$  is the energy level in the center of tile  $m$  and  $N$  is the dimension of  $\mathbf{R}_c$ . Next, we make an estimate of the clutter plus noise covariance matrix appropriate for tile  $m$ ,

$$\mathbf{R}_m = \beta_m \mathbf{R}_c + \sigma^2 \mathbf{I}. \quad (10)$$

Finally, we compute an adaptive weight vector with diagonal loading. Using an adaptive matched filter (AMF) [9] normalization the adaptive weight vector for tile  $m$  is,

$$\mathbf{w}_m = \frac{[\mathbf{R}_m + \delta \mathbf{I}]^{-1} \mathbf{v}}{\sqrt{\mathbf{v}^H [\mathbf{R}_m + \delta \mathbf{I}]^{-1} \mathbf{v}}}. \quad (11)$$

where  $\mathbf{v}$  is the space-time steering vector and  $\delta$  is diagonal loading level.

To illustrate the benefits of PVT we processed the same Tuxedo data processed in Section 3. Figure 12 shows the output power after the power variable STAP strategy. Notice that clutter reflections from rooftops visible in Figure 4 are effectively eliminated in Figure 12. Furthermore, Figure 13 depicts the output of the detection operation following power variable training. Notice there are significantly fewer false alarms in Figure 13 relative to Figure 5.

## 6. MULTI-CHANNEL ADAPTIVE SAR

In recent work at Lincoln Laboratory, researchers have explored a multi-channel adaptive SAR processing approach for detecting moving targets in SAR images [3]. This technique was demonstrated using data collected with a UHF antenna array testbed. It consists of first forming a separate SAR image on each of the antenna array channels. From these SAR images, data vectors are generated by concatenating identical pixels in range and cross-range from each channel in the antenna array. Next, a set of training vectors is identified that surrounds a given set of test vectors. The training vectors are used to estimate a covariance matrix of the background clutter and noise  $\hat{\mathbf{R}}$ . The test vectors, denoted  $\mathbf{x}(r, c)$ , are used with  $\hat{\mathbf{R}}$  to compute the change detection statistic that is compared to a threshold

$$\mathbf{x}(r, c)^H \hat{\mathbf{R}}^{-1} \mathbf{x}(r, c) > T \quad (12)$$

All threshold crossings are identified as potential targets. The covariance estimation is then repeated with such potential targets excised from the training and change detection

is repeated. In this manner the effect of target self-nulling is reduced.

This multi-channel adaptive SAR procedure produced impressive results with the UHF testbed data in [3]. The work is general enough so that it is applicable to other multi-channel radar systems that have the ability to implement long dwells with wide bandwidth waveforms. However, there are a few open issues that should be addressed before adopting this approach. First, note that the change detection statistic is invariant to array calibration errors, as it does not require a steering vector. For well-calibrated arrays the adaptive matched filter (AMF) approach outperforms the change detection approach. Therefore, with increasing levels of calibration there is a crossover point at which the performance of the AMF approach outperforms the change detection approach. Another issue is related to the computational cost associated with SAR image formation. The results in [3] implemented complete SAR image formation with polar-reformatting for each phase center on the antenna array. Implementing this approach on a real-time processor would be challenging. Furthermore, for shorter CPIs (on the order of a second) and narrower bandwidths (around 50 MHz) it may be possible to implement simpler processing (relative to SAR image formation on each phase center) at a much lower computational cost with minimal loss in performance.

## 7. EXTENDED ARRAY RECEIVER

The extended array receiver concept is not new but can provide GMTI performance benefits at the cost of additional radar hardware. In this concept separate orthogonal waveforms are simultaneously transmitted from each channel in the antenna array. The entire antenna array is used on receive and separate parallel signal processing streams are used to pulse compress the individual orthogonal waveforms. Once pulse compressed, returns from the orthogonal waveforms are coherently combined.

The benefits of this approach are easily understood with the series of plots in Figures 14, 15 and 16. If the entire antenna array is used for transmit and receive then the two-way beam pattern is narrow but only in a small coverage area, illustrated in Figure 14. To overcome the coverage issue some radar systems spoil the transmit beam to illuminate a wider area. A number of different receive beams can be simultaneously formed, as shown in Figure 15. However, in this approach the two-way beam patterns have been broadened.

The extended array receiver concept enables forming two-way beam patterns, as shown in Figure 16, which are just as narrow as those in Figure 14. But these beam patterns are all available simultaneously, as in Figure 15, because they are determined by how we choose to process the

received data.

There are several open issues with the extended array receiver concept. First, this approach assumes that multiple waveforms, approximately orthogonal over delay and Doppler, can be synthesized. In practice it may not be practical to generate waveforms that are nearly orthogonal. Therefore, we need to investigate how nearly orthogonal the waveforms need to be. As a result of using waveforms that are not strictly orthogonal the receiver noise floor will be elevated. Another issue is related to the processing hardware architecture. Pulse compressing multiple orthogonal waveforms on each channel of the receiver can be a daunting task. As part of our architecture study Lincoln Laboratory will evaluate several options to meet the demands for this application. Finally, the ability to synchronize the orthogonal waveforms for proper coherence needs to be examined.

## 8. SUMMARY

Detecting ground vehicles is challenging in real-world applications. Modern GMTI systems are plagued with excessive false alarms, missed target detections (slow moving vehicles), dense target scenarios and heterogeneous clutter environments. This paper explored several approaches to improve GMTI performance that include: moving target focusing for long CPIs, excision of training data far from the clutter ridge, power variable training without overnulling, multi-channel adaptive SAR and an extended array receiver concept. Our results illustrate improved detection performance of low Doppler targets using moving target focusing and significant improvements in false alarms with power variable training. In ongoing research Lincoln Laboratory will explore the open issues associated with multi-channel adaptive SAR and the extended array receiver concept.

## 9. REFERENCES

- [1] J. Ward, "Space-Time Adaptive Processing for Airborne Radar," *MIT Lincoln Laboratory Technical Report 1015*, 1994.
- [2] D. Rabideau and A. Steinhardt, "Improved adaptive clutter cancellation through data-adaptive training," *IEEE Transactions on Aerospace and Electronic Systems*, vol. 35, pp. 879-891, 1999.
- [3] A. Yegulalp, "FOPEN GMTI using multi-channel adaptive SAR," *Proceedings of the Adaptive Sensor Array Processing Workshop*, March 2002.
- [4] D. Kreithen, N. Pulsone, C. Rader and G. Schrader, "The MIT Lincoln Laboratory KASSPER Algorithm Testbed and Baseline Algorithm Suite," *Proceedings of*

*the Sensor Array and Multichannel Signal Processing Workshop, August 2002.*

- [5] N. L. Owsley, "Enhanced Minimum Variance Beamforming," in *Underwater Acoustic Data Processing*, Editor Y. Chan, Kluwer Academic Publishers, 1989.
- [6] C. D. Richmond, "Statistical Performance Analysis of the Adaptive Sidelobe Blanker Detection Algorithm," *Conference Record of the Thirty-First Asilomar Conference on Signals, Systems and Computers*, 1997.
- [7] J. Jao, "Theory of synthetic aperture radar imaging of a moving target," *IEEE Transactions on Geoscience and Remote Sensing*, vol. 39, pp. 1984-1992, 2001.
- [8] S. M. Kogon and M. A. Zatman, "STAP Adaptive Weight Training using Phase and Power Selection Criteria," *Conference Record of the Thirty-Fifth Asilomar Conference on Signals, Systems and Computers*, 2001.
- [9] F. C. Robey, D. R. Fuhrmann, E. J. Kelly and R. A. Nitzberg, "A CFAR Adaptive Matched Filter Detector," *IEEE Transactions on Aerospace and Electronic Systems*, vol. 28, pp. 208-216, 1992.
- [10] J. R. Fienup, "Detecting Moving Targets in SAR Imagery by Focusing," *IEEE Transactions on Aerospace and Electronic Systems*, vol. 37, pp. 794-808, 2001.

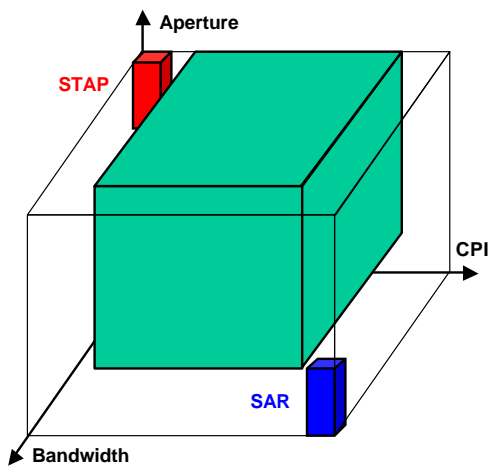


Figure 1: Radar Processing Modes: GMTI and SAR

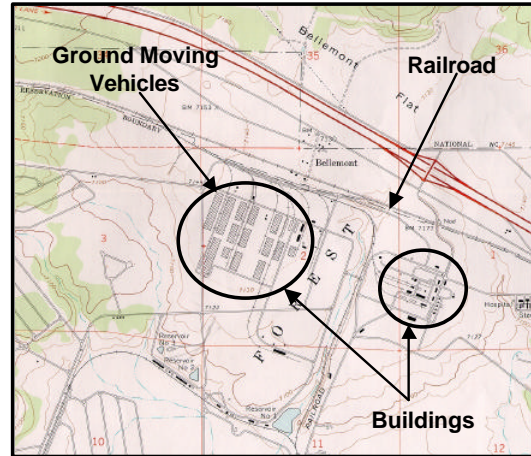


Figure 2: Camp Navajo, Arizona

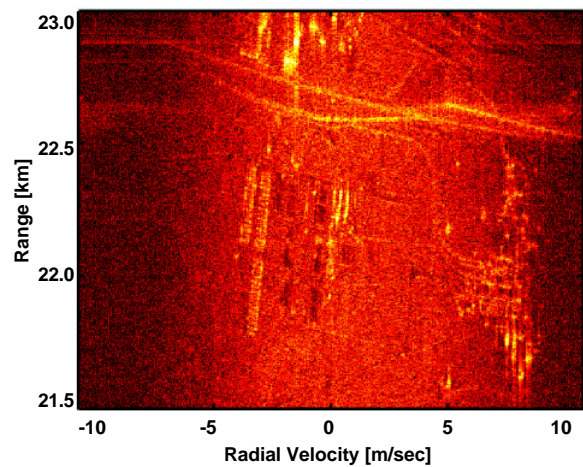


Figure 3: Tuxedo data after Doppler processing in the Baseline GMTI processing stream

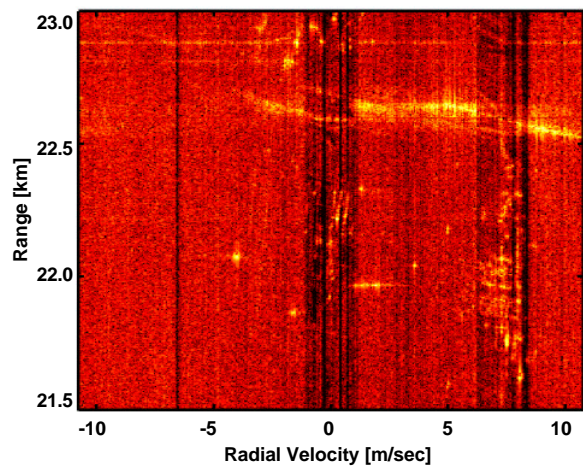


Figure 4: Tuxedo data after the STAP operation in the Baseline GMTI processing stream

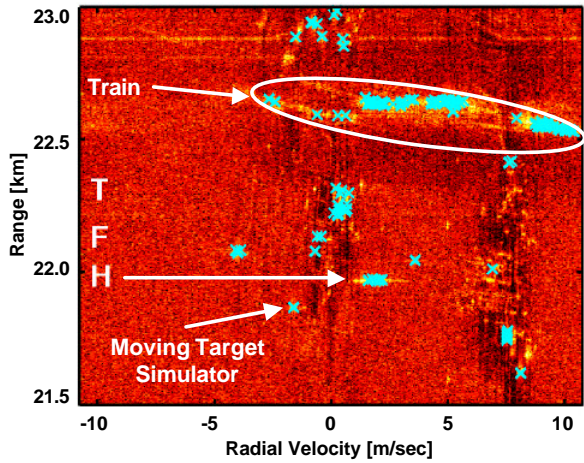


Figure 5: Tuxedo data after detection processing in the Baseline GMTI processing stream

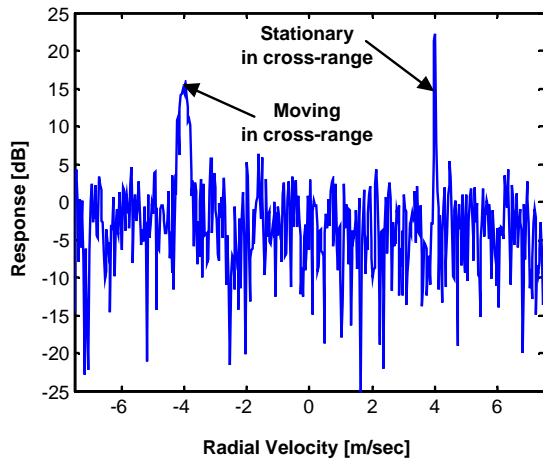


Figure 6: Processed assuming no motion in cross-range

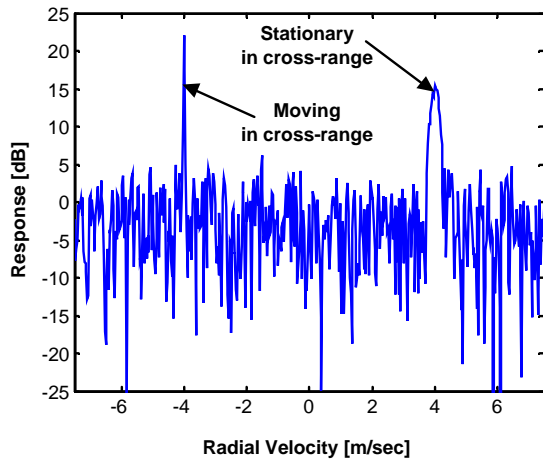


Figure 7: Processed with correction for motion in cross-range

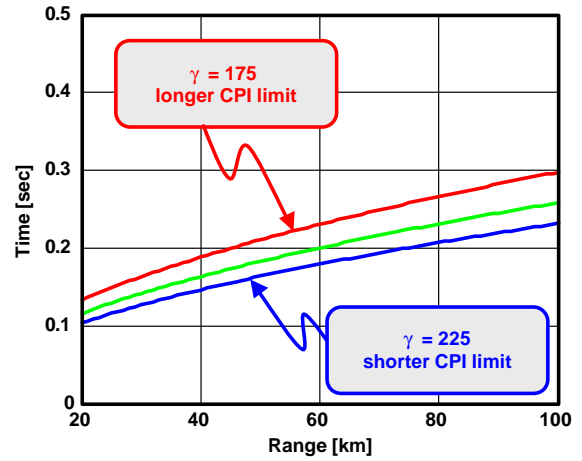


Figure 8: Limit on CPI time,  $T$ , to prevent Doppler walk

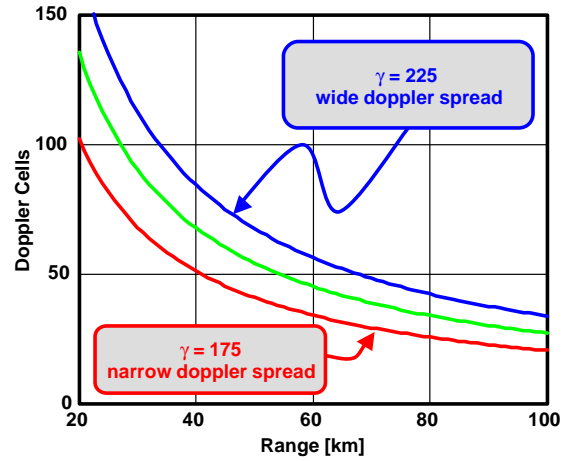


Figure 9: Number of Doppler resolution cells a broadside target traverses in one second

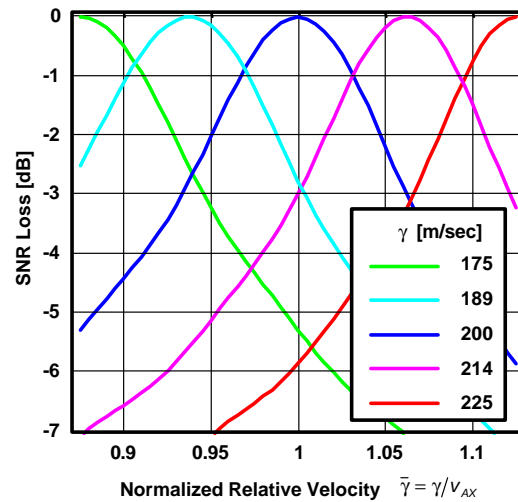


Figure 10: The response of a bank of focusing filters

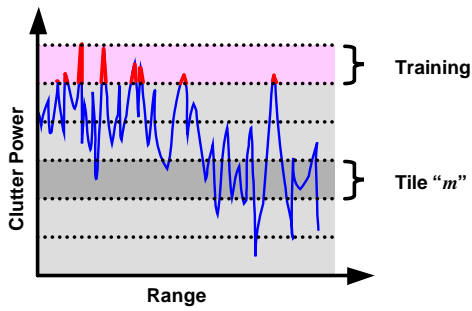


Figure 11: Power variable training

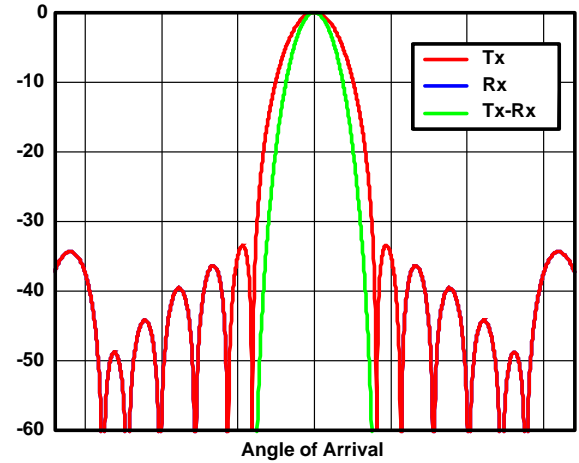


Figure 14: Full aperture on transmit and receive

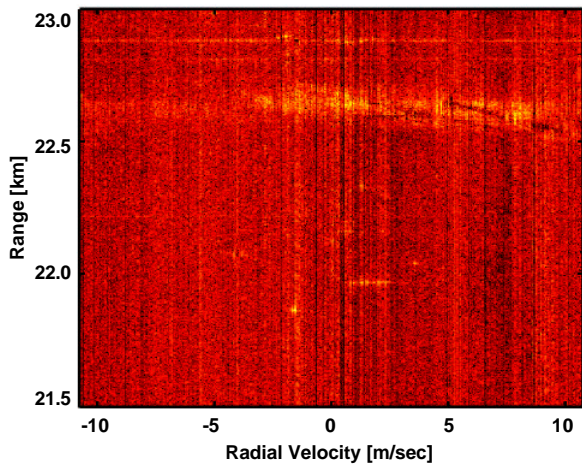


Figure 12: Tuxedo data after performing the power variable training STAP operation

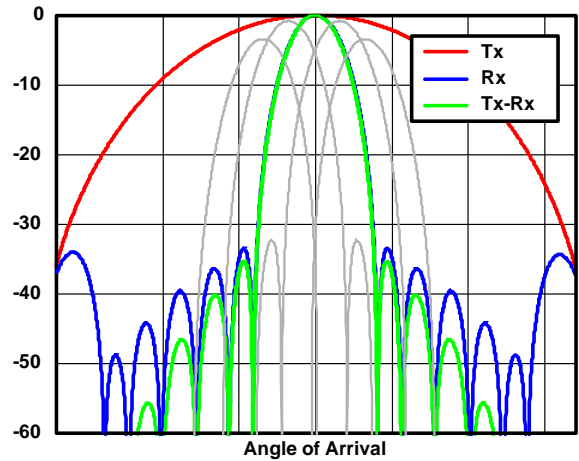


Figure 15: Sub-aperture on transmit and full aperture on receive

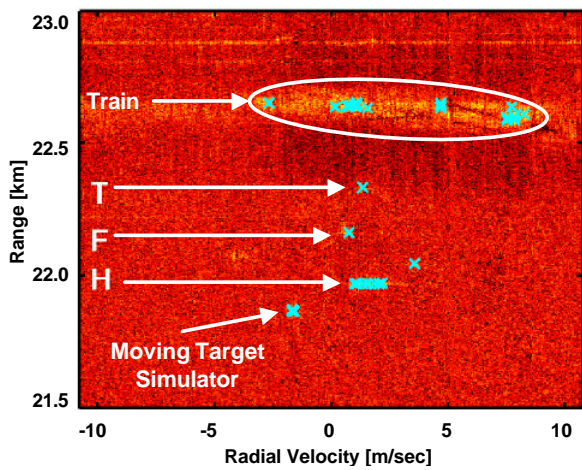


Figure 13: Tuxedo data after performing the power variable training STAP operation and detection processing

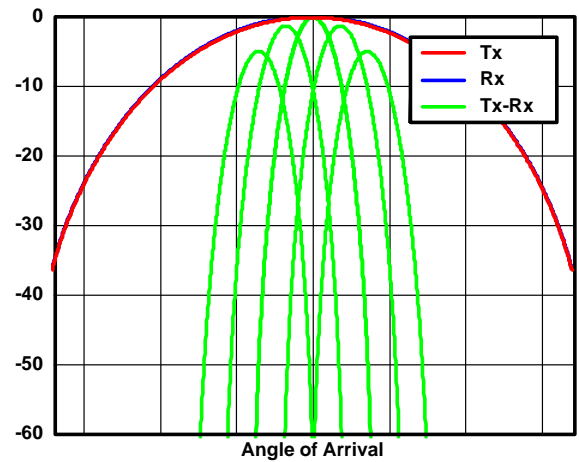


Figure 16: Extended Array Receiver